Title
MODELS FOR KINETICS OF SOLID STATE SINTERING

Author
Wong, Boon

Publication Date
1977-08-01

Submitted to American Ceramic Society

MODELS FOR KINETICS OF SOLID STATE SINTERING

Boon Wong and Joseph A. Pask

August 1977

Prepared for the U. S. Department of Energy
under Contract W-7405-ENG-48

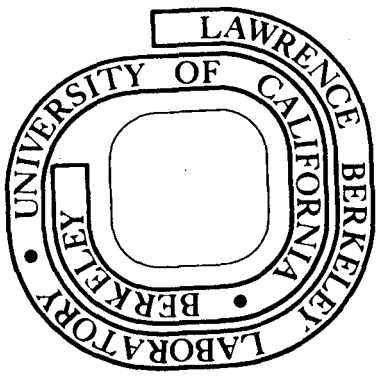

DISCLAIMER

MODELS FOR KINETICS OF SOLID STATE SINTERING

Boon Wong* and Joseph A. Pask

Materials and Molecular Research Division, Lawrence Berkeley Laboratory
and Department of Materials Science and Mineral Engineering,
University of California, Berkeley, California 94720

ABSTRACT

Kinetic equations for the isothermal densification of a single phase powder compact are formulated for the initial and intermediate stages of sintering; these are identified as continuous open pore stages, with a decreasing number of voids and grains per unit volume accompanied by grain growth occurring in the latter. Each stage can be represented by one of two equations: one based on mass transport along the forming grain boundary to the "neck" region as the rate controlling step, and one on movement from the neck to the free surface regions as the rate controlling step.

*Based on part of a thesis submitted by Boon Wong for the Ph.D. degree in Materials Science at the University of California, Berkeley. Now at GTE Laboratories (Sylvania) Waltham, Mass.

I. INTRODUCTION

Solid state sintering is the critical step in the fabrication and development of ceramic, metallic and polymeric materials. It is a high temperature process during which a powder compact generally shrinks and decreases its pore volume, and increases its bulk density. From a thermodynamic point of view, solid state sintering is a thermally activated process during which an assembly of particles of equilibrium chemical composition decreases its total interfacial free energy by a larger decrease in the total solid-vapor interfacial energy relative to the total increase of the solid-solid interfacial, i.e. grain boundary, energy in the system by means of mass transport mechanisms. Therefore, the driving force for the process is this reduction of the total interfacial energy of the system.[1]

Normally, the goal of solid state sintering is to develop at the lowest possible temperature a dense polycrystalline material with a controlled microstructure. In order to achieve this goal, an understanding of the fundamentals of the process is essential. This paper presents some models and derives kinetic equations for different isothermal sintering stages and conditions. A separate paper[2] presents an experimental application of the derived equations to the sintering of an MgO powder.

II. NATURE OF SOLID STATE SINTERING

The solid state sintering process during which shrinkage occurs can be divided into three stages: initial, intermediate and final.[1] The formation of a framework of particles by formation of grain boundaries at particle contacts has been occasionally referred to in the literature as the initial stage, but it will be here classified as the preliminary

stage. This stage is also being identified on the basis of any rearrangement of particles that may occur as the framework forms. Little, if any, shrinkage occurs due to mass transport processes.

The initial and intermediate stages of crystalline particle compacts are identified by the presence of continuous open pore channels with no change in the number of voids occurring in the former and a decreasing number of voids per unit volume in the latter. These stages are also identified on the basis of no grain growth and grain growth, respectively. The final stage is identified as the closed pore stage; grain growth invariably occurs during this stage. Grain growth also generally continues with continued heating after the system reaches theoretical or endpoint density.

The decrease in the number of voids and grain growth in the intermediate stage occurs in real systems because of the presence of a range of particle and aggregate sizes, nonhomogeneity of packing, and anisotropy of interfacial energies. Thus, in an ideal system of uniform size spheres with isotropic surface and grain boundary energies that are packed uniformly, no intermediate stage would exist. In real system clumps, aggregates and agglomerates with denser packing relative to the whole system densify first because of their smaller voids; with the closing of voids, larger particles form and the distances between remaining voids increase. The respective lengths of the initial and intermediate periods are therefore dependent on the character of the powder. In some cases, the initial stage may be so short as to essentially merge with the preliminary stage.

Detailed analyses of sintering during the open pore periods have been presented in the literature by a number of workers.[3-11] Coble made a critical analysis and presented diffusion models for the initial (as defined here) and final stages.[10,12] Improper identification of stages and mass transport mechanisms have undoubtedly contributed to the differences in kinetic studies that have appeared in the literature.

In this discussion kinetic equations are derived for the initial and intermediate stages of sintering as defined. The models are all-important. In this case a two-step mass transport mechanism or process is used: (1) material moves along the grain boundary to the solid/vapor/solid dihedral angle or "neck" regions, and (2) then to the free surface regions. For each of the stages, depending on the experimental conditions, either step (1) or (2) can be the slow step in the mass transport and thus control the kinetics although shrinkage always occurs by the step (1) mechanism. It is thus logical that different equations should be needed to represent each of the four conditions.

III. THERMODYNAMIC CONSIDERATIONS OF SINTERING

The change in free energy during sintering of a powder compact at chemical composition equilibrium can be expressed as

$$\delta G_{sys} = \delta \int \gamma_{sv} dA_{sv} + \delta \int \gamma_{ss} dA_{ss} \qquad (1)$$

where G_{sys} is the total interfacial energy of the system, γ_{sv} represents the specific surface free energies, and γ_{ss}, specific interfacial or grain boundary energies, A_{sv} is the free surface area, and A_{ss} is the interfacial area. The first term is negative since the surface areas decrease, and the second term is positive since the grain boundary areas

increase. As long as the net change in free energy for the system at any instant (δG_{sys}) is negative, a driving force for sintering exists.

This concept can be illustrated by a model of two spheres with an interface, as shown in Fig. 1. Ideal multisphere models utilize the same densification concept but each particle has more contacts or developing grain boundaries, the number being dependent on the packing of the particles; attention is then directed to the voids whose structure is dependent on the packing of particles. The growth of the grain boundary areas and resultant shrinkage in all cases is realized by the indicated two step mass transport process. The geometry of the neck region is determined by whether step (1) or (2) is the slow step. Figure 1A illustrates the ideal configuration that results when step (1) is the slow step; and Fig. 1B, when step (2) is the slow step. The driving force for mass transport for step (1) results from a chemical potential gradient establighes by the existence of non-equilibrium dihedral angles, and for step (2) by reverse curvature in the surfaces in the neck region.

The Fig. 1A configuration represents an ideal condition in which the reverse curvature does not develop due to a faster step (2) which maintains a minimum free surface area; the dihedral angle under these conditions starts at 0° and increases until the equilibrium dihedral angle is reached which would correspond to equilibrium shrinkage and minimum surface area as determined by Eq. (1) when δG_{sys} becomes zero. The equilibrium dihedral angle at this point can be expressed by

$$\frac{\gamma_{ss}}{\gamma_{sv}} = 2 \cos \frac{\Phi}{2} . \qquad (2)$$

During continuing shrinkage, however, it can be seen that Φ starts at

0° and increases until Φ_{eq} is reached; the corresponding transient value for the left term starts at 2 and decreases until the value for $(\gamma_{ss}/\gamma_{sv})_{eq}$ is reached, which is represented in Eq. (1). A thermodynamic driving force for mass transport by step (1) then exists as long as the dihedral angle is not at equilibrium, and can be expressed as

$$\delta G_{sys} \propto 2 \left(\cos \frac{\Phi_{eq}}{2} - \cos \frac{\Phi}{2} \right). \qquad (3)$$

δG_{sys} becomes zero in both Eqs. (1) and (3) when the equilibrium dihedral angle is reached; no further shrinkage then occurs.

The Fig. 1B configuration represents a condition in which a neck with an equilibrium dihedral angle builds up quickly and is maintained due to a faster step (1). The resulting reverse curvature of the free surface in the neck region becomes the source of the thermodynamic driving force for mass transport in step (2) than controls the kinetics. The resulting mass transport to remove the curvature causes Φ_{eq} to be upset which immediately is brought back to equilibrium by a faster step (1) process. When the reverse curvature is eliminated, the equilibrium Fig. 1A configuration is reached and no further shrinkage occurs.

IV. PHENOMENOLOGICAL VISCOUS CONCEPT FOR SOLID STATE SINTERING KINETICS

Mass transport along the grain boundary region to the neck (step 1) and from the neck along the free surface region (step 2) is due to chemical potential gradients set up because of nonequilibrium conditions and normally visualized and expressed as vacancy gradients. The mass transport or diffusion is phenomenologically equivalent to viscous shear

flow. Since such flow or diffusion takes place at every contact point in the compact, it can be related to the bulk shrinkage of the whole compact.

Regardless of the detailed mechanisms, when a porous isotropic viscous solid is under uniform pressure and at a constant temperature, the rheological equation derived, based on the law of conservation of energy,[13] is

$$\zeta \left(\frac{dV}{Vdt}\right) = - \sum_{i=1}^{n} \sigma_i \tag{4}$$

where the right side of the equation is the algebraic sum of the pressures (capillary pressures, external, etc.) on the solid, ζ is bulk viscosity, V is total specific bulk volume of the porous compact, and t is time. Since

$$V = \frac{V_S}{1-P} \tag{5}$$

where V_S is specific true volume of the material and P is fractional porosity, differentiating Eq. (5) with respect to time, we have

$$\frac{dV}{dt} = V_S \, (1-P)^{-2} \, \frac{dP}{dt}. \tag{6}$$

Substituting Eq. (6) and Eq. (5) into Eq. (4), we have

$$\zeta \, \frac{1}{(1-P)} \, \frac{dP}{dt} = - \sum_{i=1}^{n} \sigma_i. \tag{7}$$

According to Skorokhod,[14] the bulk viscosity of a porous viscous material can be expressed in terms of porosity and the effective shear viscosity, η, along the active grain boundaries as

$$\zeta = \frac{4}{3} \eta \, \frac{(1-P)}{P} \tag{8}$$

for all values of P. Upon substitution of Eq. 8 into Eq. 7 we obtain the general phenomenological sintering kinetic equation:

$$\frac{4}{3}\eta\frac{1}{P}\frac{dP}{dt} = -\sum_{i=1}^{n}\sigma_i. \qquad (9)$$

V. ASSUMED GEOMETRY FOR THE MODELS

In determining mass transport by diffusion or shear flow, it is necessary to take into account variations in vacancy concentration gradients that the controlling mass transport step is dependent upon. These are dependent upon the distances of movement along the contact planes or grain boundaries during step (1) which increase with shrinkage and along the free surface regions during step (2) which can conveniently be expressed in terms of grain size and porosity.

It is assumed that the individual grains will have a uniform average size and an average shape. The developing shape during the initial stage is determined by the degree of packing or the number of contacts that an individual particle has. The ultimate final shape formed by grain boundary motion is represented by the polyhedron tetrakai-decahedron which is a truncated octahedron with 14 faces, 36 edges and 24 corners, as shown in Fig. 2, because it has the smallest interfacial area in a polycrystalline compact for a given grain size. The configuration is formed directly, and thus most readily by a starting body-centered cubic packing of uniform-sized spheres; the 8 near neighbor contacts for a given sphere cause its conversion to an octahedron shape which transforms to the truncated shape when contacts are made with the 6 second neighbors and closed pores develop representing

the final stage. The development of sintering equations is based on this configuration.

Coble[10] showed that the relationship between the volume of the polyhedron, V_{poly}, its edge length, ℓ_p, and average grain size, G, can be expressed as

$$V_{poly} = 8\sqrt{2}\ell_p^3 = \frac{4}{3}\pi\left(\frac{G}{2}\right)^3 = 0.52G^3. \tag{10}$$

During the open pore stages, it is assumed for calculation purposes that the pores or voids are essentially cylinders lying along the to-be three-grain edges of the polyhedrons. The volume of cylindrical pores associated with each grain can be expressed as

$$V_{cyl} = 13.5\ G\ r_c^2 \tag{11}$$

where r_c is the radius of the cylindrical pore. Therefore, the porosity during the open pore stages is

$$P = \frac{V_{cyl}}{V_{poly}} = \frac{13.5\ G\ r_c^2}{0.52\ G^3} = 26\ \frac{r_c^2}{G^2} \tag{12}$$

or

$$r_c = 0.2G\ P^{1/2}. \tag{13}$$

VI. SINTERING KINETICS

Sintering equations for the initial and intermediate stages are developed on the basis of whether step (1) or step (2) of the mass transport process is the kinetic controlling step as outlined in Section II. The basic transport mechanism for a given controlling step is

essentially the same for the two stages. The distinction between the initial and intermediate stages is the initiation of grain growth, or decrease in number of voids, in the latter with maintenance of some continuous open pores. Grain growth results in a condition where the number of active grain boundary contacts and voids or pores per unit bulk volume decrease with a corresponding decrease in fractional bulk volume shrinkage rate.

A. Step (2) Controlled Kinetics

In this case a dynamic equilibrium dihedral angle is formed at the solid/vapor/solid triple line in the neck during the preliminary stage. The resulting inverse curvature in the free surface as seen in Fig. 1B provides the controlling driving force for sintering by establishing a vacancy concentration gradient between the free surface and the neck regions:[3,15]

$$\Delta C \simeq \frac{2C_o \Omega \gamma_{sv}}{kTr_c} \tag{14}$$

where C_o is the vacancy concentration on a flat surface, Ω is atomic (molecular) volume, k is Boltzmann's constant, r_c is the cylindrical radius of the pore, and T is absolute temperature. Multiplying both sides of Eq. (14) by $6D_v/2\pi r_c$ results in the following flux equation between the free surface and neck regions:

$$J \simeq \frac{2D_v C_o \Omega \gamma_{sv}}{kTr_c^2} \simeq \frac{2D_B \gamma_{sv}}{kTr_c^2} \tag{15}$$

where D_v is the vacancy diffusion coefficient, and D_B is the bulk

diffusion coefficient since $D_B = D_v C_o \Omega$ and $J = 3D_v \Delta C/2\ r_c$ where $2\pi r_c/6$ is the diffusion path.

The creep rate will then approximately be:

$$\dot{\varepsilon} = \frac{-4J\Omega}{\ell_p} \simeq \frac{-8D_B \Omega \gamma_{sv}}{kTr_c^2\ \ell_p} \simeq \frac{-22D_B\Omega}{kTr_c G}\left(\frac{\gamma_{sv}}{r_c}\right) \tag{16}$$

since, from Eq. (10), $\ell_p = 0.36G$. From Eq. (16), the corresponding effective shear viscosity coefficient η can be expressed as:

$$\eta = \frac{kTr_c G}{22D_B\Omega} \tag{17}$$

Substituting Eq. (17) into Eq. (9) and rearranging, results in the equation:

$$\frac{1}{P}\left(\frac{dP}{dt}\right) = \frac{-17D_B\Omega}{kTr_c G} \sum_{i-1}^{n} \sigma_i . \tag{18}$$

If it is assumed that during the initial stage of sintering $\Sigma\sigma_i = \gamma_{sv}/r_c$ and substituting Eq. (13) into Eq. (18), with rearrangement of terms, we obtain

$$\frac{dP}{dt} = \frac{-425D_B\Omega\gamma_{sv}}{kTG^3} = \frac{-A_1 D_B \Omega \gamma_{sv} N^3}{kT} . \tag{19}$$

where A_1 is a proportionality constant, and N is the number of interconnected voids per unit volume and inversely proportional to G, the grain size, which also determines the number of grains per unit volume for a given packing. For the initial stage of sintering then Eq. (19)

can be integrated to give

$$(P-P_o) = \frac{-A_1 D_B \Omega \gamma_{sv} N^3}{kT} (t-t_o). \qquad (20)$$

Although the derivation of and the constant terms in this equation are different from that of Coble's equation,[10] the indication of a linear densification rate is the same.

During the intermediate stage in real systems, grain growth and a corresponding reduction of number of voids or pores interconnected by channels or grain boundaries occur due to the presence of a range of particle sizes and nonuniform packing of particles and agglomerates. It is postulated that the reduction of the number of voids follows a cubic law represented by $N^3 = \frac{1}{mt}$ where m is a time-independent coefficient. Substituting this relationship in Eq. (19) and integrating, we obtain

$$(P-P_o) = \frac{-A_1 D_B \Omega \gamma_{sv}}{mkT} \ln\left(\frac{t}{t_o}\right). \qquad (21)$$

B. Step (1) Controlled Kinetics

In this case, the dihedral angle at the solid/vapor/solid triple line in the neck increases as sintering proceeds. If in a multisphere compact the equilibrium angle is reached according to the model in Fig. 1A before complete densification of the system is reached because of a sufficiently large value for $(\gamma_{ss}/\gamma_{sv})_{eq}$, the system reaches an end point density. The existence of the nonequilibrium angle during sintering provides the driving force for densification because of the establishment of a vacancy concentration gradient along the grain boundary from its center to the triple point line due to tension at the triple line and

compression at the center according to Nabarro[16] and Herring.[17] Using the thermodynamic driving force expressed in Eq. (3) in the format of Eq. (14), ΔC becomes

$$\Delta C \simeq \frac{2C_o\Omega}{kT}\left(\frac{2\gamma_{sv}\left(\cos\frac{\Phi}{2} - \cos\frac{\Phi_{eq}}{2}\right)}{r_c}\right) \tag{22}$$

Since $D_{gb} = D_{gbv}C_o\Omega$, the flux of material becomes:

$$J \simeq \frac{4D_{gb}\omega}{kt}\left(\frac{\gamma_{sv}\left(\cos\frac{\Phi}{2} - \cos\frac{\Phi_{eq}}{2}\right)}{r_c}\right) \tag{23}$$

where D_{gb} is grain boundary diffusion coefficient, D_{gbv} is grain boundary diffusion coefficient of vacancies, and ω is the grain boundary width.

The creep rate due to material flow along grain boundaries, considering that $\ell_p^3 = 0.046G^3$ according to Eq. (10), then is

$$\dot{\epsilon} = \frac{-36J\Omega}{(3)8\sqrt{2}\ell_p^3} = \frac{-43D_{gb}\omega\Omega}{kTG^3}\left(\frac{2\gamma_{sv}\left(\cos\frac{\Phi}{2} - \cos\frac{\Phi_{eq}}{2}\right)}{r_c}\right). \tag{24}$$

From Eq. (24) the effective shear viscosity coefficient η can be expressed as

$$\eta = \frac{kTG^3}{43D_{gb}\omega\Omega}. \tag{25}$$

The relationship between Φ and P during the open pore stage when the porosity of the green or unfired compact is assumed to be 0.54 is[11]

$$\frac{\Phi}{2} \simeq \left(0.36 - 0.49P^{1/2}\right). \tag{26}$$

Using Eq. (26) and arbitrarily assuming $\Phi_e = 140°$ for oxides we obtain

$$\sigma_c \simeq \frac{2\gamma_{sv}\left[\cos\left(0.36 - 0.49P^{1/2}\right) - 0.34\right]}{r_c}. \tag{27}$$

Mathematical treatment of Eq. (27) results in

$$\sigma_c \simeq \frac{2\gamma_{sv}\left(0.60 + 0.17P^{1/2} - 0.12P\right)}{r_c}. \tag{28}$$

Substituting Eqs. (25) and (28) into Eq. (9), using the relationship of Eq. (13) for r_c, and substituting N for G as in Eq. (19), we obtain

$$\left[\frac{1}{P^{1/2}\left(0.60 + 0.17P^{1/2} - 0.12P\right)}\right]\frac{dP}{dt} = \frac{-A_2 D_{gb}\omega\Omega_{sv} N^4}{kT}. \tag{29}$$

For the initial stage of sintering when N remains essentially constant Eq. (20) can be integrated to give

$$\left[\tanh^{-1}\left(-0.43P^{1/2} + 0.3\right) - \tanh^{-1}\left(-0.43P_o^{1/2} + 0.3\right)\right] = \frac{A_3\gamma_{sv}D_{gb}\omega\Omega N^4}{kT}(t-t_o). \tag{30}$$

During the intermediate stage with the occurrence of grain growth and reduction of number of voids, substituting the relationship of $N^3 = 1/mt$ into Eq. (29) and integrating, we obtain

$$\left[\tanh^{-1}\left(-0.43P^{1/2} + 0.3\right) - \tanh^{-1}\left(-0.43P_o^{1/2} + 0.3\right)\right] = \frac{-A_4\gamma_{sv}D_{gb}\omega\Omega}{kTm^{4/3}}\left(\frac{1}{t^{1/3}} - \frac{1}{t_o^{1/3}}\right) \tag{31}$$

where A_2, A_3 and A_4 are constants.

The numerical values in Eq. (30) and (31) are based on the selection of $\Phi_{eq} = 140°$ and an unfired porosity of 0.54 which were considered to be approximate average values. Other values for these parameters will change the numerical factors in the equations with a shift of the positions of the curves plotted as the porosity function versus the time parameter. The slopes of the straight line portions for each of these equations, however, will not change.

VII. SUMMARY

Three stages have been identified in the densification process: initial, intermediate, and final.[1] In the real systems, particularly with low unfired bulk densities, a preliminary stage can be identified in which some rearrangement of particles occurs before grain boundaries are formed. Continuous open porosity is maintained in the first two stages, with grain growth and decrease of number of voids or pores interconnected by channels or grain boundaries occurring in the intermediate stage. Only closed pores are present in the final stage. The grain growth, and decrease of numbers of grains and voids, identifying the intermediate stage occurs only in real systems due to the presence of a range of particle and aggregate sizes and nonuniformity of packing. The respective lengths of the preliminary, initial and intermediate stages are dependent on the character and packing characteristics of the powders. Grain growth upon pore closures and subsequent annealing is due to anisotropy of surface and grain boundary energies, curvature of grain boundaries, and nonequilibrium solid/solid/solid dihedral angles formed during the sintering process.

Kinetic equations for the isothermal densification of a single phase powder compact are based on the slow or controlling step of the mass transport process. In all cases the mass transport process is divided into two steps: movement of material along the particle/particle contact or grain boundary to the neck regions, and then movement from the neck to the free surface regions.[1]

Kinetic equations have been formulated for the initial and intermediate stages of isothermal sintering for cases when step (1) (Eqs. 30 and 31) and when step (2) (Eqs. 20 and 21) were the rate controlling steps in the mass transport process. Experimental verification of these equations is being published in another paper.[2]

ACKNOWLEDGMENT

This work was supported by the Division of Materials Sciences, Office of Basic Energy Sciences, U.S. Department of Energy.

REFERENCES

1. J. A. Pask, C. E. Hoge and B. Wong, Dependence of Sintering Characteristics on Thermodynamic and Geometric Factors, Chapter in Ceramic Microstructures '76, edited by Richard M. Fulrath and Joseph A. Pask, Westview Press, Boulder, CO, pp. 246-254, 1976.
2. B. Wong and J. A. Pask, Experimental Analysis of Sintering of MgO Compacts, submitted to J. Am. Ceram. Soc.
3. G. C. Kuczynski, Self-Diffusion in Sintering of Metallic Particles, Trans. AIME, 185, 169 (1949).
4. J. Frenkel, Viscous Flow of Crystalline Bodies Under the Action of Surface Tension, J. Physics (U.S.S.R.), 9 [5] 385 (1945).
5. W. D. Kingery and M. Berg, Study of Initial Stages of Sintering Solids by Viscous Flow, Evaporation - Condensation, and Self-Diffusion, J. Appl. Physics, 26, 1205 (1955).
6. R. L. Coble, Initial Sintering of Alumina and Hematite, J. Am. Ceram. Soc., 41, 55 (1958).
7. D. L. Johnson and I. B. Cutler, Diffusion Sintering: Initial Stage Sintering Models and Their Application to Shrinkage of Powder Compacts, J. Am. Ceram. Soc., 46, 541 (1963).
8. D. L. Johnson and T. M. Clarke, Grain Boundary and Volume Diffusion in the Sintering of Silver, Acta Met., 12, 1173 (1964).
9. D. L. Johnson, New Method of Obtaining Volume, Grain-boundary and Surface Diffusion Coefficients from Sintering Data, J. Appl. Physics, 40, 192 (1969).
10. R. L. Coble, Sintering Crystalline Solids: I, Intermediate and Final State Diffusion Models, J. Appl. Physics, 32, 787 (1961).

11. B. Wong, Kinetics and Mechanisms of Single Phase Solid State Sintering, Ph.D. Thesis, LBL-3957, University of California, August 1975.

12. R. L. Coble, Sintering Crystalline Solids: II. Experimental Test of Diffusion Models in Powder Compacts, J. Appl. Physics, 32, 793 (1961).

13. M. S. Koval'chenko and G. V. Samsonov, Application of Viscous Flow Theory to the Question of Sintering Powders by Hot Pressing, Poroshkovaya Met., No. 2,3 (1961).

14. V. V. Skorokhod, On the Phenomomenological Theory of Densification or the Sintering of Porous Bodies, Poroshkovaya Met., No. 2, 14 (1961).

15. G. C. Kuczynski, Measurement of Self-Diffusion of Silver Without Radioactive Tracers, J. Appl. Phys., 21, 632 (1950).

16. F. R. N. Nabarro, Deformation of Crystals by Motion of Single Ions, Report of a Conference on the Strength of Solid, The Physical Society, London, P. 75 (1948).

17. C. Herring, Diffusional Viscosity of a Polycrystalline Solids, J. Appl. Phys., 21, 437 (1950).

FIGURES

1. Two-sphere ideal models with isotropic interfacial energies: (A) minimum free energy geometric configuration when step (1) is rate controlling for mass transport, and (B) neck formation configuration with maintained equilibrium dihedral angle when step (2) is rate controlling.
2. Model of tetrakaidecahedron or truncated octahedron shape assumed by uniform size spherical particles in body-centered cubic packing after complete densification with no grain growth.

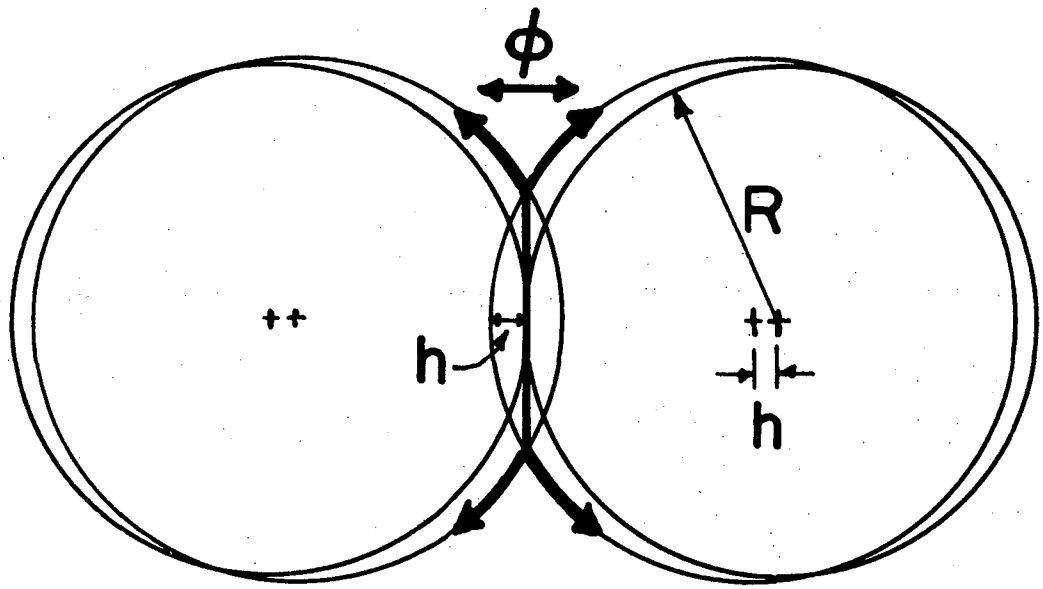

$$dG = \gamma_{SV}\, dA_{SV} + \gamma_{GB}\, dA_{GB}$$

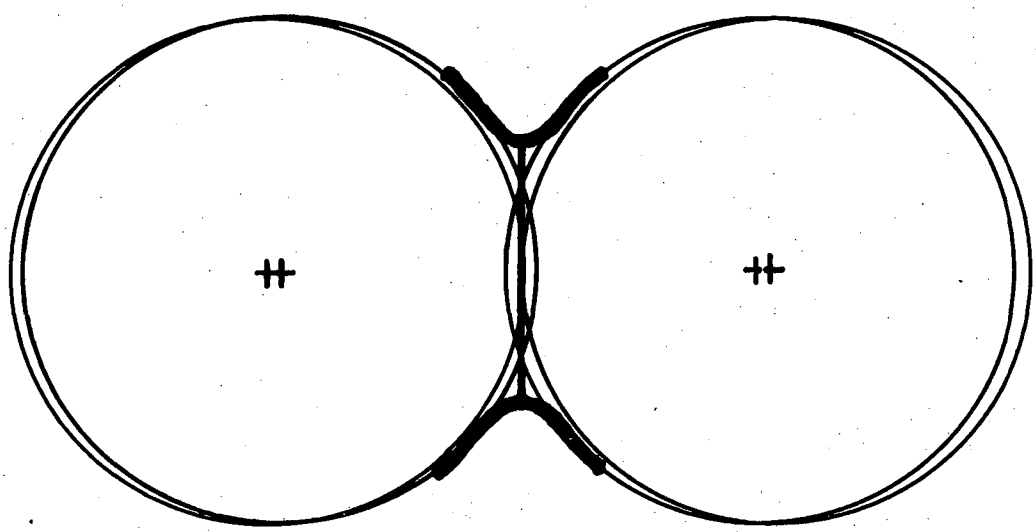

$$\gamma_{GB} = 2\,\gamma_{SV} \cos \phi/2$$

XBL 789-5743

Fig. 1

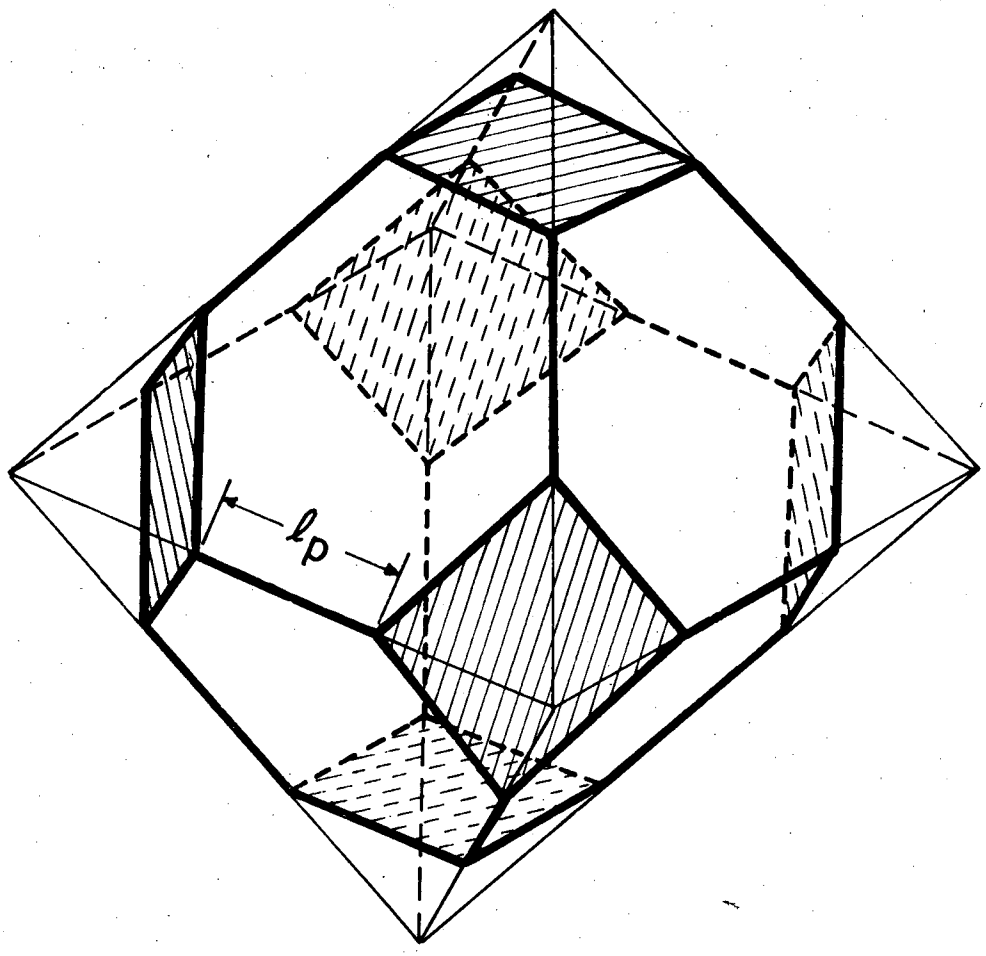

XBL 773-5228

Fig. 2

TECHNICAL INFORMATION DEPARTMENT
LAWRENCE BERKELEY LABORATORY
UNIVERSITY OF CALIFORNIA
BERKELEY, CALIFORNIA 94720